Online ^{13}C and ^{14}C gas measurements by EA-IRMS–AMS at ETH Zürich

Cameron P. McIntyre[1,2,3], Lukas Wacker[2], Negar Haghipour[1], Thomas M. Blattmann[1], Simon Fahrni[2,4], Muhammed Usman[1], Timothy I. Eglinton[1], Hans-Arno Synal[2].

[1]Biogeoscience, ETH Zürich, NO, Sonnegstrasse 5, 8092, Zürich, Switzerland.
[2]Laboratory of Ion Beam Physics, ETH Zürich, HPK, Otto-Stern-Weg 5, 8093 Zürich, Switzerland.
[3]Current address: SUERC AMS Laboratory, University of Glasgow, Rankine Av., G75 0QF, Glasgow, UK.
[4]Current address: Ionplus AG, Lerzenstrasse 12, 8953 Dietikon, Switzerland.

Corresponding author: cameron.mcintyre@glasgow.ac.uk

1. Abstract

Studies using carbon isotopes to understand the global carbon cycle are critical to identify and quantify sources, sinks and processes and how humans may impact them. ^{13}C and ^{14}C are routinely measured individually, however, there is a need to develop instrumentation that can perform concurrent online analyses that can generate rich datasets conveniently and efficiently. To satisfy these requirements, we coupled an elemental analyser to a stable isotope mass spectrometer and an accelerator mass spectrometer system fitted with a gas ion source. We first tested the system with standard materials and then reanalysed a sediment core from the Bay of Bengal that had been analysed for ^{14}C by conventional methods. The system was able to produce %C, ^{13}C and ^{14}C data that was accurate and precise, and suitable for the purposes of our biogeochemistry group. The system was compact and convenient and is suitable for use in a range of fields of research.

2. Introduction

Paired ^{13}C and ^{14}C measurements have become an essential part of a tiered, integrated analytical methodology for biogeoscience and global carbon cycle studies. Stable $^{13}C/^{12}C$ isotope ratios are typically used to discriminate between sources such as marine and terrestrial plant carbon while $^{14}C/^{12}C$ ratios add temporal and apportionment capabilities through the radioactive decay of ^{14}C (Hedges et al. 1997; Megens et al. 2001; Reddy et al. 2002). With a half-life of 5730 years ^{14}C is particularly useful for studies concerning earth's recent history during the Holocene. Recent studies utilising carbon isotopes have been able to identify and quantify crucial carbon cycle processes such as the transfer of terrestrial carbon to the ocean and its burial (Vonk et al. 2014; Mann et al. 2015; Tao et al. 2015). This has lead to significant improvements to our understanding of the earth's natural processes and the impact of humans.

The measurement of ^{13}C and ^{14}C individually is now routine and established. Stable isotope ratio mass spectrometers (IRMS) can measure $^{13}C/^{12}C$ ratios to

50 better than 0.1 permil (‰) precision which is sufficient for biogeochemical
51 samples that typically span a range of 60 permil with respect to their deviation
52 from the Pee Dee Belemnite standard ($\delta^{13}C$ VPDB) (Polissar et al. 2009). The
53 abundance of ^{14}C is, however, only one part in a trillion and therefore requires an
54 accelerator mass spectrometer (AMS) to achieve the required overall system
55 efficiency and the elimination of isobars and interferences such as ^{14}N and ^{13}CH
56 (Synal et al. 2007). Measurement of $^{14}C/^{12}C$ ratios typically spans a range from
57 modern atmospheric levels to ancient ^{14}C free samples corresponding to a
58 fraction modern ($F^{14}C$) from 1 to 0. A precision of ± 2 ‰ is routinely achievable
59 for the modern standard oxalic acid II (NIST SRM 4990C) and the detection limit
60 is typically less than $F^{14}C$ 0.002 (52 ka BP). The technique is now readily
61 accessible to scientists however still comparatively intensive with respect to cost
62 and instrumentation (Wacker et al. 2010b; Wacker et al. 2010c).
63
64 At this point it is important to highlight that in an AMS laboratory the ^{13}C content
65 of a sample is additionally used as a correction parameter for the ^{14}C content
66 (Donahue et al. 1990; Reimer et al. 2004). This is an important concept whereby
67 the isotopic fractionation of ^{14}C from natural processes occurs at a rate
68 approximately twofold that of ^{13}C and that fractionation must be corrected for so
69 that ^{14}C can be used on a uniform time scale.
70
71 Due to the design of sputter ion sources, AMS systems are not as precise as IRMS
72 systems and thus measurements for the sample ^{13}C and ^{14}C corrections are
73 typically made on separate systems. In some laboratories, offline IRMS sample
74 $\delta^{13}C$ is used for a retroactive ^{14}C correction calculations however, where
75 possible, it is considered preferable to use concurrent $^{13}C/^{12}C$ data obtained from
76 the AMS during measurement since part of the fractionation that has to be
77 corrected for is induced in the sputter ion source itself (Santos et al. 2007;
78 Prasad et al. 2013). Due to the reasons outlined above, the arrangement of
79 instrumentation in AMS laboratories can occur in several ways.
80
81 Conventional AMS measurements use samples prepared as solid graphite and a
82 caesium sputter ion source to produce high intensity carbon ion beams. To
83 convert non-gaseous samples to graphite they are first converted to CO_2 by
84 combustion or acid decomposition and subsequently reduced with hydrogen
85 over an Fe catalyst (Vogel et al. 1984). A portion of the CO_2 gas can be diverted
86 and measured using an IRMS for a high precision $\delta^{13}C$ with the remainder of the
87 sample graphitised. The ^{13}C content of the graphite can then be measured by the
88 AMS system and used for fractionation correction purposes. Hence we find
89 laboratories that have IRMS systems integrated online and offline with their
90 graphitisation systems (Gagnon et al. 2000; Hong et al. 2010; Kato et al. 2014).
91
92 AMS systems can also be fitted with a gas ion source whereby the samples are
93 introduced directly as CO_2 gas as an alternate mode of operation (Ramsey et al.
94 2004; Fahrni et al. 2013). Here it is possible to analyse small samples but, due to
95 reduced system efficiencies, the measurement precision is typically reduced to
96 1% or better for a modern sample (Ruff et al. 2010a). The advantage however is
97 that direct coupling of interfaces such as an elemental analyser (EA) and/or an
98 IRMS is possible which can improve productivity where moderate precision ^{14}C

measurements are acceptable (Ruff et al. 2010b; Wacker et al. 2013; Braione et al. 2015; Salazar et al. 2015). This fits well with biogeochemical studies that seek to understand global processes and have large sample sets requiring high precision ^{13}C and moderate precision ^{14}C data.

In this study we outline the features of our integrated, online, gas accepting ion source, EA-IRMS-AMS system in routine use at ETH Zürich. For sediment and soil samples from the biogeochemistry group, we have moved away from graphite preparation and separate IRMS and AMS measurement to routine online measurements that are adequately precise for the group's studies and goals. Our first goal was to construct a high performance, compact, automated system to increase productivity and convenience. The second goal was to be able to analyse 20 mg of Holocene sediment or soil containing typically 1 wt% organic carbon for $\delta^{13}C$ with precision of better than ± 0.1‰ VPDB and $F^{14}C$ with a precision of better than ± 1%.

3. Experimental

3.1 System description

The system is comprised of an elemental analyser (vario MICRO cube, Elementar) and a stable isotope ratio mass spectrometer (visION, Isoprime) connected to a gas interface system (GIS, Ionplus) and a Mini CArbon Dating Sytem (MICADAS, Ionplus) (Figure 1). Connecting tubing was 1/16" stainless steel and additional 4-port and 6-port switching valves were used to provide multiple modes of operation between the various interfaces and mass spectrometers (Figure S1). This way, for example, the EA-IRMS system could be used standalone while the AMS was being used with a carbonate handling system (CHS, Ionplus) or an ampoule cracker. The footprint of the interfaces was 2 m x 1 m and fitted alongside the MICADAS system.

The IRMS we selected has an internal backpressure controller that is used to split the flow from the EA between the IRMS source and IRMS vent. The vent of the IRMS was connected to the GIS and the backpressure controller set such that 10% of the gas flowing from the EA went to ion source of the IRMS and the remaining 90% was trapped for AMS analysis. The backpressure controller provided the additional benefit of maintaining a constant pressure of gas to the IRMS while the GIS trap was actuating and heating.

3.2 Calibration of standards

Standards selected for EA-IRMS-AMS were oxalic acid II (NIST SRM 4990C), phthalic anhydride (Sigma, PN-320064-500g, LN-MKBH1376V), atropine (Säntis, PN - SA990746B, LN- 51112) and acetanilide (Merck, PN-100011, LN - K37102211229). 500 ± 50 µg C each were loaded into 5 x 8 mm tin foil capsules (Säntis) and analysed by conventional EA-IRMS for $\delta^{13}C$ VPDB against the primary standards IAEA-CH3, -CH7 and -CH6. Atropine and acetanilide are

147 additionally elemental analysis standards while oxalic acid and phthalic
148 anhydride are ^{14}C isotope standards.
149
150 The EA was operated in CN analysis mode with the method modified to include
151 an additional column burn off step at the end of the analysis where the internal
152 gas adsorption column used for separating CO_2 and N_2 column is heated to 200
153 °C before cooling to 50 °C. 25mm quartz tubes were used with the CuO
154 combustion tube set to 920 °C and the Cu reduction tube at 550 °C. The
155 combustion tube was packed with 5mm quartz wool, 10 mm quartz chips, 5mm
156 quartz wool, 50 mm silver wool, 5mm quartz wool, 65 mm CuO wire and 3mm
157 corundum balls. Al_2O_3 wool was used in the ash finger. Standards were
158 combusted using an 80 s injection of supplementary oxygen at 30 mL/min. The
159 elemental data was processed separately using the vario MICRO software.
160
161 The IRMS method was a standard CN method modified to monitor carbon only
162 with monitoring gas injected for 2 x 30 s before and after the CO_2 peak of
163 interest. Data was processed separately using the IonOS software.
164
165 3.3 EA-IRMS-AMS analysis of standards
166
167 Eight replicates of 50-150 ug C of oxalic acid II, phthalic anhydride, acetanilide,
168 atropine, IAEA-C6, and IAEA-C8 were weighed into tin foil capsules. They were
169 run in order sorted firstly from blank to modern and secondly from large to
170 small. Three additional phthalic anhydride blanks were run at the end after the
171 IAEA-C6 to assess system memory. The IRMS was operated in a standalone mode
172 with the method based on timed events and a single start trigger inputted from
173 GIS software.
174
175 The AMS was run in gas mode and configured to run with the EA and GIS using a
176 method modified to incorporate the IRMS (Ruff et al. 2010b; Fahrni et al. 2013).
177 The timing schedule begins with the start trigger sent to EA and IRMS and had a
178 total runtime of 15.5 minutes per sample which gave a precision of <1 % on a
179 single oxalic acid standard. The zeolite trap of the GIS was cooled to 10 °C for
180 trapping and heated to 450 °C for desorption. Data was processed separately
181 using BATS software (Wacker et al. 2010a) and oxalic acid (NIST SRM4990C) and
182 phthalic anhydride were used for calibration of both ^{13}C and ^{14}C data.
183
184 3.4 EA-IRMS-AMS analysis of a sediment core
185
186 Sediment core NGHP-01-16A core was collected from the Bay of Bengal in 2006
187 as part of the Indian National Gas Hydrate Program (Collett et al. 2014) and
188 radiocarbon analysis of foraminifera has been previously conducted (Ponton et
189 al. 2012). The core was stored frozen at the Woods Hole Oceanographic
190 Institution and sub-sampled at 3 cm interval from 20 - 750 cm. Samples were
191 packed in dry ice and shipped to ETH Zürich where they were fumigated in 8 x 8
192 x 15 mm silver boats (Elementar) with HCl to remove carbonate (Komada et al.
193 2008) and neutralized for 24 hrs at 60 °C over solid NaOH to remove residual
194 acid. The samples were wrapped in a second 8 x 8 x 15 mm tinfoil boat
195 (Elementar) and pressed prior to analysis.

Fumigated samples were analysed for ^{14}C via conventional solid graphite. Graphite samples containing 1 mg C were prepared using an AGE 3 system (Ionplus) and analysed using a MICADAS system (Ionplus). Samples were normalised using oxalic acid II (NIST SRM4990C) and anthracite coal as a blank. Secondary standards were IAEA-C7 and -C8. Data was processed using BATS software (Wacker et al. 2010a).

Samples were then run as gas and were prepared to contain 200 -500 μg C. The samples were split into groups of 17 and bracketed by 200 μg C standards and blanks. We began and finished the run with oxalic acid and phthalic anhydride and separated the groups with 3 oxalic acids and 1 atropine. The runtime was shortened to 13.6 min and the standards were combusted in the EA with 80 s of supplementary oxygen while the samples had 120 s. The GIS has a capacity of 100 μg C and auto-split mode is used to reduce the size of the sample before dilution and injection into the AMS.

4. Results and Discussion

4.1 Calibration of standards

The results of the calibration of the standards for $\delta^{13}C$ VPDB using the standalone EA-IRMS system are given in Table S1. No significant drift was observed however we used a multipoint correction for offset (Coplen et al. 2006). The results show that the IRMS is able to measure standards to a precision of 0.05 ‰ or better for n=4-8. This is more than sufficient for the specification of our group of 0.1 ‰ and n = 4-8 standards are suitable for a typical AMS run. The value we determined for oxalic acid II was -17.69 ± 0.03 ‰ which fell within error of the high precision IRMS value report by Schneider et al. (1995) of -17.68 ± 0.02 ‰ (Schneider et al. 1995). Our value is higher than the consensus value used by AMS laboratories of -17.8 ‰ however it is well within the range of values reported by Mann (1983) (Mann 1983) that were used to determine the consensus value. We have adopted the more precise IRMS value of Schneider et al. (1995) for use in our laboratory. By calibrating these materials we have a robust set of standards that can be used to collect %C, %N, C/N, ^{13}C and ^{14}C data depending on the requirements of the analysis.

4.2 EA-IRMS-AMS analysis of standards

The results of the analysis of standards by EA-IRMS-AMS are given in Table 1. The results presented here are from the first run of the system. Again, the standards were measured precisely for ^{13}C and all of them fell within error of the consensus values at the 2σ level. Atropine was anomalously lower than the consensus value in this run and we were unable to explain this atypical result or improve it by performing the offset correction with additional standards.

We observed no crosstalk or systematic shifts in the acquired ^{13}C ratios based on the mass of the sample which showed the IRMS system could be operated with

samples containing as little as 50 µg C. The EA-AMS system has been characterised for operation down to 5 µg C and preliminary IRMS tests indicate it can be operated between 5-50 µg C with data correction (data not shown). Between 5 and 50 µg C is the range at which extraneous carbon begins to have a noticeable effect and requires correction for constant contamination and crosstalk (Shah and Pearson 2007; Ruff et al. 2010b; Santos et al. 2010; Salazar et al. 2015).

Similarly the ^{14}C data for the acetanilide, atropine, IAEA-C8 and IAEA-C6 was within error of the consensus values at the 1σ level. The oxalic acid standards were each measured to 8 ‰ producing a mean value with 3 ‰ precision (n=8) and a scatter of 2 ‰. The blank value was typical for this system and corresponded to background of $F^{14}C$ 0.0046 ± 0.0012 (43 ka BP). System blanks are dependent on the carbon content of the EA capsules used, memory, crosstalk and ion source cleanliness. The data for the standards was corrected for a constant contamination of 0.5 µg C with a $F^{14}C$ of 0.6 which is typical for the capsules we use (Ruff et al. 2010b).

In this analysis we ran three additional blanks after the 8 replicates of IAEA-C6 to study an extreme case of crosstalk. The $F^{14}C$ decreased sequentially from 0.0133 to 0.0065 and then 0.0042 and shows what we typically experience, which is that the EA and GIS system shows < 1% crosstalk and that we can return to background levels after 2 samples. Crosstalk in interfaces is unavoidable and we have mitigation procedures to minimise this limitation. Choice of capsule size and material has been shown to have a first order effect (Ruff et al. 2010b), and after that we consider the running order of samples and the preparation methods. The calibration and tuning procedure starts with oxalic acid followed by blanks until stable values are obtained then samples are run in order from ancient to modern to minimise the crosstalk. Pre-conditioning steps such as EA and trap 'burn off' have been used in EA-AMS systems (Salazar et al. 2015) and unknown samples could easily be rerun during the sequence. In this way we can minimise or omit the application of correction procedures for subtracting crosstalk from previous samples. Development is on going to reduce the crosstalk in the GIS system.

4.3 EA-IRMS-AMS analysis of a sediment core

The results from the EA-IRMS-AMS analysis of the Bay of Bengal core are shown in Figures 2, 3 and 4. Fully detailed data will be presented and interpreted in a future thesis and publication. The samples analysed fall within the working range of the EA (0-3 mg C) and of the IRMS (200-700 µg C) for high precision measurements. Comparison of the EA and GIS data showed that 90% of the sample CO_2 generated by the EA was trapped by the GIS. This was equal to the split ratio of the IRMS and indicates that the GIS was able to trap all of the CO_2 gas delivered to it from the IRMS for sample sizes up to 470 µg C. The GIS however is typically operated at a 100 µg C capacity (at 4% CO_2 in helium), so it automatically reduces the quantity of the trapped CO_2 to 100 µg C prior to dilution with He and injection into the AMS. Any isotopic fractionation of the CO_2 occurring during the trapping and splitting steps is corrected for by the AMS ^{13}C

293 measurement and fractionation correction in ^{14}C data reduction (Donahue et al.
294 1990).
295
296 Using the EA it is possible to obtain %C, %N and C/N during analysis however in
297 this study we only collected data for %C. By incorporating a secondary standard
298 such as atropine into the run we have additional calibration points for elemental
299 analysis and ^{13}C. The precision of the %C measurements was 2% RSD based on
300 n=16 oxalic acid standards which is more than sufficient for our requirements.
301 Normally, unless prior knowledge of the %C content of the samples is available,
302 we perform an initial screening run with the EA so that we can set the size of the
303 samples to fit within the working range of the system. An additional limitation of
304 this study was that the IRMS system was not configured for auto dilution of the
305 samples and as a result the sample sizes needed to be within a relatively narrow
306 carbon range and we could not capture ^{15}N for these sediment samples, which
307 had a relatively low N content.
308
309 The data for ^{13}C content is clearly superior from the IRMS and the precision was
310 0.1 ‰ for oxalic acid (n=21), 0.06‰ for phthalic anhydride (n=13) and 0.09 ‰
311 for atropine (n=6) (Fig. 3). It shows that as little as n=6 standards can be used
312 however we include more so that we can monitor drift in the IRMS and AMS
313 systems. In figure 3 we additionally show data for ^{13}C acquired by the AMS
314 during graphite (B) and gas (C) analysis. The data is sample-averaged data and is
315 used for the instantaneous online correction of the ^{14}C data. The scatter of the
316 data shows that it is not reliable for use as the accurate $\delta^{13}C$ VPDB of the sample.
317 This highlights the importance of obtaining a separate stable isotope
318 measurement by IRMS for this purpose. It should be noted however that these
319 data are acquired using the prototype MICADAS system and that the latest
320 MICADAS systems are capable of obtaining better quality ^{13}C data.
321
322 The data for the ^{14}C content showed that 46/47 of the samples analysed using
323 solid graphite and CO_2 gas fall with error of each other at the 2σ level, confirming
324 that the gas ion source can be used to generate accurate data (Figure 4). This
325 core has previously been analysed for foraminiferal ^{14}C and the ages from 11
326 carbonate samples were younger by up to a thousand years. The shift is
327 consistent for the different sources of the samples (organic vs. inorganic C) and
328 will be interpreted in a future publication nonetheless the foramifera data
329 supports the ages found in this study. In this run the precision and scatter of the
330 oxalic acid standards was 2 ‰ and the precision of the samples was 10 ‰. In
331 these samples there was enough carbon to double the measurement time and
332 precision however we accepted the shorter run time preferentially. The
333 precision and blank of the graphite data was 5 ‰ and $F^{14}C$ 0.006 (40 ka BP), and
334 for the gas was 10 ‰ and $F^{14}C$ 0.015 (33 ka BP). The background was elevated
335 in the gas run, as the ion source required cleaning.
336
337 The accuracy of the gas data could be further improved by applying a correction
338 for an assumed constant contamination and crosstalk however we did not run
339 processing controls in this batch and can only perform a speculative correction.
340 The gas and graphite data show the best match when a correction for constant
341 contamination of 6 µg C with a $F^{14}C$ of 0.9 is performed. This mass and $F^{14}C$ is

342 considered moderately high but not unreasonable for the large tin boats and
343 fumigation procedure we use. A consequence of the correction is that the error is
344 approximately doubled for the gas samples due to the propagation of the errors
345 and the larger influence on and smaller sample sizes. In order for the corrections
346 to be applied rigorously, processing controls must be run with each batch of
347 samples.
348
349
350 4.4 Practical aspects to operation of the system
351
352 The primary advantage of the system was its integration, flexibility and
353 throughput. The ability to operate the system in several modes either as the full
354 EA-IRMS-AMS system or as independent systems such as CHS-AMS and EA-IRMS,
355 standalone EA and standalone AMS with ampoule cracker, meant that capacity
356 wastage was minimised. In full system mode it is possible to run continuously
357 with the only intervention required being changing the cathode magazine every
358 40 cathodes and performing EA maintenance. EA maintenance to change the ash
359 finger or reduction tube could be done in less 10 min with the IRMS and AMS
360 paused. We were able to routinely run batches of more than 50 samples
361 overnight with the main limitation being staff hours. It is worth noting that the
362 start up of the full system was relatively time consuming due to the use of 4
363 individual components (EA, IRMS, GIS, AMS) and was not practical for small
364 batches.
365
366
367 5. Conclusions
368
369 The EA-IRMS-AMS system described in this paper was able to meet the specified
370 requirements for the analysis of soils and sediments in our biogeochemistry
371 group. The system was able to analyse 20 mg of modern sediment or soil
372 containing 1 wt.% organic carbon for $\delta^{13}C$ with precision of better than ± 0.1 ‰
373 and ^{14}C with an $F^{14}C$ precision of better than ± 1%. It was additionally able to
374 obtain % organic carbon with an RSD of 2 %. The system was also capable of
375 analyzing samples containing less than 100 µg C although further validation
376 experiments are required for small samples containing 5-100 µg C. Careful
377 analysis of processing controls are required to quantify the addition of
378 extraneous carbon and to correct for constant contamination and crosstalk. The
379 system has been able to increase the productivity of our group and has allowed
380 us to move away from conventional preparation of graphite for these types of
381 samples. The system is a high performance, compact, automated (with
382 supervision) system that would be suitable for use in other fields such as
383 archaeology, paleoclimatology, soil science, biomedicine and forensics.
384
385
386 6. Acknowledgements
387
388 This work is supported by funding from the SNF and the authors would like to
389 thank Adam Sookdeo for help with preparation of the standards. The authors
390 wish to thank Paul Wheeler, Mike Sudnik and Graham Entwistle at Isoprime for

their help with the installation, operation and programming of the IRMS. Thanks to Liviu Gioson at WHOI for supplying the core from the Bay of Bengal.

7. Figure Captions

Figure 1. Schematic of the EA-IRMS-AMS system for online paired 13C and 14C gas measurements. Samples are combusted in an elemental analyser (EA) and the product CO_2 is transferred to a stable isotope ratio mass spectrometer (IRMS) for high precision ^{13}C measurement. 90% of the gas is split internally by the IRMS and sent to the accelerator mass spectrometer system (AMS) for ^{14}C measurement. Details of the gas interface system and EA-IRMS can be found in Ruff et al. (2010).

Table 1. Analysis of standards by EA-IRMS-AMS. Oxalic acid and phthalic anhydride are calibration standards for both ^{13}C and ^{14}C.

Figure 2. Plot of total organic carbon (TOC) vs. depth as determined by EA-IRMS-AMS for sediment samples taken from a core from the Bay of Bengal. The relative error based on n = 16 oxalic acid standards was 2%.

Figure 3. ^{13}C analysis by EA-IRMS-AMS of sediment samples from a core from the Bay of Bengal. A) IRMS data with a precision of <0.1 ‰. B) AMS graphite data. C) AMS gas data using a gas ion source.

Figure 4. ^{14}C analysis by EA-IRMS-AMS of sediment samples from a core from the Bay of Bengal. Green triangles are conventional solid graphite data and blue circles are data from CO_2 using a gas ion source. Data from 46/47 gas samples are within error of the graphite samples at the 2 sigma level. The single missing data point was due to a bad cathode. For comparison, red squares are conventional graphite ^{14}C values for foraminifera from Ponton et. al , 2012.

Table S1. Calibration of standards. Plotting measured values versus consensus for the IAEA standards gave a linear least squares fit with the equation y = 1.0152x - 0.0582 (R^2 =1) which was used to correct the unknowns for offset.

Figure S1. Schematic of the valve arrangement. Vici Valco 4-port and 6-port valves (0.75mm bore) are used to connect the carbonate handling system (CHS) and the elemental analyser (EA) to the IRMS and AMS systems. Separate systems can then be operated concurrently. GIS (AMS) refers to the input of the GIS box.

8. References

Braione E, Maruccio L, Quarta G, D'Elia M, Calcagnile L. 2015. A new system for the simultaneous measurement of delta C-13 and delta N-15 by IRMS and radiocarbon by AMS on gaseous samples: Design features and performances of the gas handling interface. Nuclear Instruments &

Methods in Physics Research Section B-Beam Interactions with Materials and Atoms 361:387-91.
Collett TS, Boswell R, Cochran JR, Kumar P, Lall M, Mazumdar A, Ramana MV, Ramprasad T, Riedel M, Sain K, Sathe AV, Vishwanath K, Party NES. 2014. Geologic implications of gas hydrates in the offshore of India: Results of the National Gas Hydrate Program Expedition 01. Marine and Petroleum Geology 58:3-28.
Coplen TB, Brand WA, Gehre M, Groning M, Meijer HAJ, Toman B, Verkouteren RM. 2006. New guidelines for delta C-13 measurements. Analytical Chemistry 78(7):2439-41.
Donahue DJ, Linick TW, Jull AJT. 1990. Isotope-Ratio and Background Corrections for Accelerator Mass-Spectrometry Radiocarbon Measurements. Radiocarbon 32(2):135-42.
Fahrni SM, Wacker L, Synal HA, Szidat S. 2013. Improving a gas ion source for C-14 AMS. Nuclear Instruments & Methods in Physics Research Section B-Beam Interactions with Materials and Atoms 294:320-7.
Gagnon AR, McNichol AP, Donoghue JC, Stuart DR, von Reden K, Nosams. 2000. The NOSAMS sample preparation laboratory in the next millenium: Progress after the WOCE program. Nuclear Instruments & Methods in Physics Research Section B-Beam Interactions with Materials and Atoms 172:409-15.
Hedges JI, Keil RG, Benner R. 1997. What happens to terrestrial organic matter in the ocean? Organic Geochemistry 27(5-6):195-212.
Hong W, Park JH, Kim KJ, Woo HJ, Kim JK, Choi HW, Kim GD. 2010. Establishment of Chemical Preparation Methods and Development of an Automated Reduction System for Ams Sample Preparation at Kigam. Radiocarbon 52(3):1277-87.
Kato K, Tokanai F, Anshita M, Sakurai H, Ohashi MS. 2014. Automated Sample Combustion and Co2 Collection System with Irms for C-14 Ams in Yamagata University, Japan. Radiocarbon 56(1):327-31.
Komada T, Anderson MR, Dorfmeier CL. 2008. Carbonate removal from coastal sediments for the determination of organic carbon and its isotopic signatures, delta C-13 and Delta C-14: comparison of fumigation and direct acidification by hydrochloric acid. Limnology and Oceanography-Methods 6:254-62.
Mann PJ, Eglinton TI, McIntyre CP, Zimov N, Davydova A, Vonk JE, Holmes RM, Spencer RGM. 2015. Utilization of ancient permafrost carbon in headwaters of Arctic fluvial networks. Nature Communications 6.
Mann WB. 1983. An International Reference Material for Radiocarbon Dating. Radiocarbon 25(2):519-27.
Megens L, van der Plicht J, de Leeuw JW. 2001. Temporal variations in C-13 and C-14 concentrations in particulate organic matter from the southern North Sea. Geochimica Et Cosmochimica Acta 65(17):2899-911.
Polissar PJ, Fulton JM, Junium CK, Turich CC, Freeman KH. 2009. Measurement of C-13 and N-15 Isotopic Composition on Nanomolar Quantities of C and N. Analytical Chemistry 81(2):755-63.
Ponton C, Giosan L, Eglinton TI, Fuller DQ, Johnson JE, Kumar P, Collett TS. 2012. Holocene aridification of India. Geophysical Research Letters 39.

Prasad GVR, Noakes JE, Cherkinsky A, Culp R, Dvoracek D. 2013. The New 250kV Single Stage AMS System at CAIS, University of Georgia: Performance Comparison with a 500kV Compact Tandem Machine. Radiocarbon 55(2-3):319-24.

Ramsey CB, Ditchfield P, Humm M. 2004. Using a gas ion source for radiocarbon AMS and GC-AMS. Radiocarbon 46(1):25-32.

Reddy CM, Pearson A, Xu L, McNichol AP, Benner BA, Wise SA, Klouda GA, Currie LA, Eglinton TI. 2002. Radiocarbon as a tool to apportion the sources of polycyclic aromatic hydrocarbons and black carbon in environmental samples. Environmental Science & Technology 36(8):1774-82.

Reimer PJ, Brown TA, Reimer RW. 2004. Discussion: Reporting and calibration of post-bomb C-14 data. Radiocarbon 46(3):1299-304.

Ruff M, Szidat S, Gaggeler HW, Suter M, Synal HA, Wacker L. 2010a. Gaseous radiocarbon measurements of small samples. Nuclear Instruments & Methods in Physics Research Section B-Beam Interactions with Materials and Atoms 268(7-8):790-4.

Ruff M, Fahrni S, Gaggeler HW, Hajdas I, Suter M, Synal HA, Szidat S, Wacker L. 2010b. On-Line Radiocarbon Measurements of Small Samples Using Elemental Analyzer and Micadas Gas Ion Source. Radiocarbon 52(4):1645-56.

Salazar G, Zhang YL, Agrios K, Szidat S. 2015. Development of a method for fast and automatic radiocarbon measurement of aerosol samples by online coupling of an elemental analyzer with a MICADAS AMS. Nuclear Instruments & Methods in Physics Research Section B-Beam Interactions with Materials and Atoms 361:163-7.

Santos GM, Moore RB, Southon JR, Griffin S, Hinger E, Zhang D. 2007. AMS C-14 sample preparation at the KCCAMS/UCI facility: Status report and performance of small samples. Radiocarbon 49(2):255-69.

Santos GM, Southon JR, Drenzek NJ, Ziolkowski LA, Druffel E, Xu XM, Zhang DC, Trumbore S, Eglinton TI, Hughen KA. 2010. Blank Assessment for Ultra-Small Radiocarbon Samples: Chemical Extraction and Separation Versus Ams. Radiocarbon 52(3):1322-35.

Schneider RJ, McNichol AP, Nadeau MJ, VonReden KF. 1995. Measurements of the oxalic acid II oxalic acid I ratio as a quality control parameter at NOSAMS. Radiocarbon 37(2):693-6.

Shah SR, Pearson A. 2007. Ultra-microscale (5-25 mu g C) analysis of individual lipids by C-14 AMS: Assessment and correction for sample processing blanks. Radiocarbon 49(1):69-82.

Synal HA, Stocker M, Suter M. 2007. MICADAS: A new compact radiocarbon AMS system. Nuclear Instruments & Methods in Physics Research Section B-Beam Interactions with Materials and Atoms 259(1):7-13.

Tao SQ, Eglinton TI, Montlucon DB, McIntyre C, Zhao MX. 2015. Pre-aged soil organic carbon as a major component of the Yellow River suspended load: Regional significance and global relevance. Earth and Planetary Science Letters 414:77-86.

Vogel JS, Southon JR, Nelson DE, Brown TA. 1984. Performance of Catalytically Condensed Carbon for Use in Accelerator Mass-Spectrometry. Nuclear Instruments & Methods in Physics Research Section B-Beam Interactions with Materials and Atoms 5(2):289-93.

536 Vonk JE, Semiletov IP, Dudarev OV, Eglinton TI, Andersson A, Shakhova N,
537 Charkin A, Heim B, Gustafsson O. 2014. Preferential burial of permafrost-
538 derived organic carbon in Siberian-Arctic shelf waters. Journal of
539 Geophysical Research-Oceans 119(12):8410-21.
540 Wacker L, Christl M, Synal HA. 2010a. Bats: A new tool for AMS data reduction.
541 Nuclear Instruments & Methods in Physics Research Section B-Beam
542 Interactions with Materials and Atoms 268(7-8):976-9.
543 Wacker L, Bonani G, Friedrich M, Hajdas I, Kromer B, Nemec M, Ruff' M, Suter M,
544 Synal HA, Vockenhuber C. 2010b. Micadas: Routine and High-Precision
545 Radiocarbon Dating. Radiocarbon 52(2):252-62.
546 Wacker L, Nemec M, Bourquin J. 2010c. A revolutionary graphitisation system:
547 Fully automated, compact and simple. Nuclear Instruments & Methods in
548 Physics Research Section B-Beam Interactions with Materials and Atoms
549 268(7-8):931-4.
550 Wacker L, Fahrni SM, Hajdas I, Molnar M, Synal HA, Szidat S, Zhang YL. 2013. A
551 versatile gas interface for routine radiocarbon analysis with a gas ion
552 source. Nuclear Instruments & Methods in Physics Research Section B-
553 Beam Interactions with Materials and Atoms 294:315-9.
554

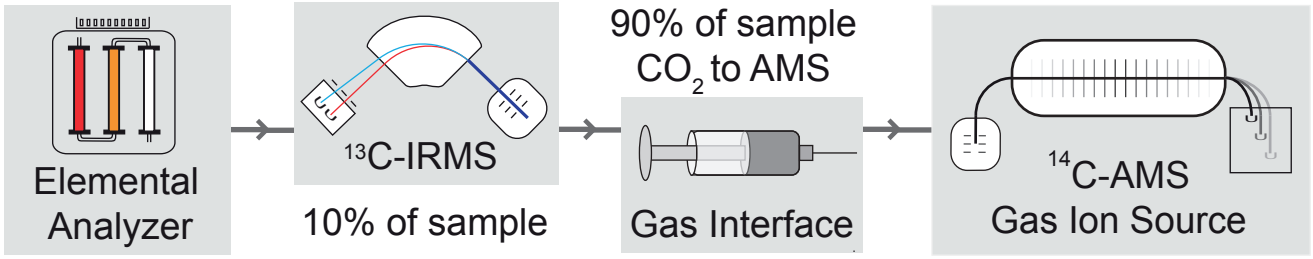

Figure 1. Schematic of the EA-IRMS-AMS system for online paired ^{13}C and ^{14}C gas measurements. Samples are combusted in an elemental analyser (EA) and the product CO_2 is transferred to a stable isotope ratio mass spectrometer (IRMS) for high precision ^{13}C measurement. 90% of the gas is split internally by the IRMS and sent to the accelerator mass spectrometer system (AMS) for ^{14}C measurement. Details of the gas interface system and EA-IRMS can be found in Ruff et al. (2010).

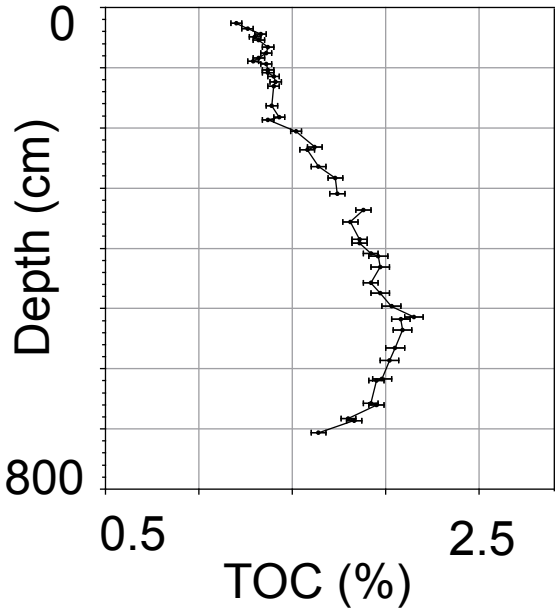

Figure 2. Plot of total organic carbon (TOC) vs. depth as determined by EA-IRMS-AMS for sediment samples taken from a core from the Bay of Bengal. The relative error based on n = 16 oxalic acid standards was 2%.

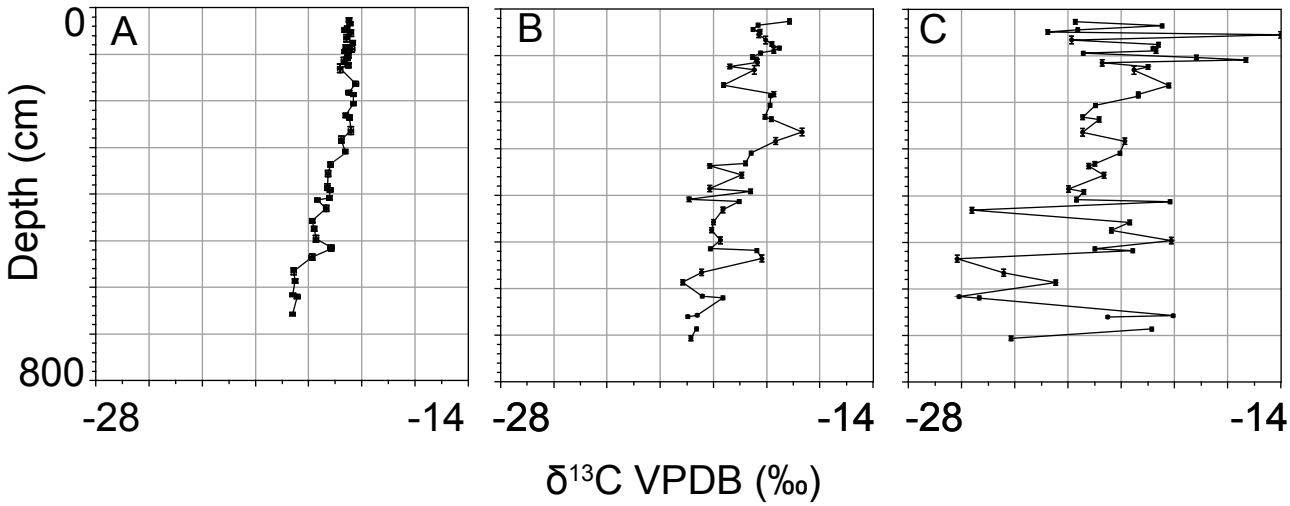

Figure 3. ^{13}C analysis by EA-IRMS-AMS of sediment samples from a core from the Bay of Bengal. A) IRMS data with a precision of <0.1 ‰. B) AMS graphite data. C) AMS gas data with a gas ion source.

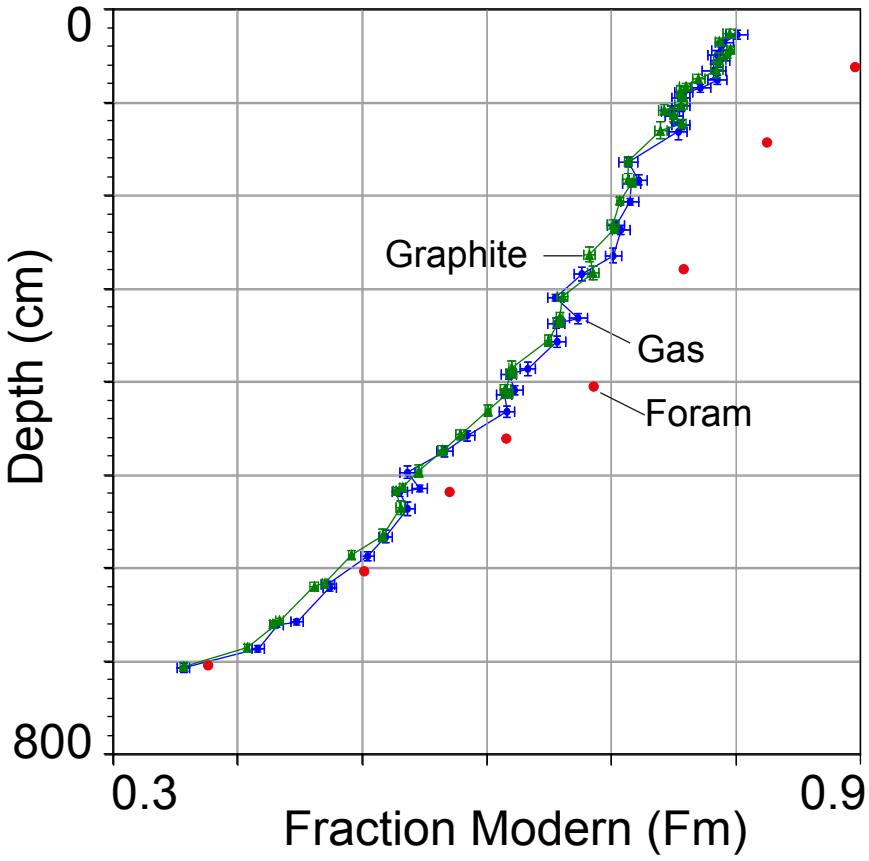

Figure 4.^{14}C analysis by EA-IRMS-AMS of sediment samples from a core from the Bay of Bengal. Green triangles are data conventional solid graphite and blue circles are data from CO_2 using a gas ion source. Data from 46/47 samples are within error at the 2 sigma level and are uncorrected for constant contamiantion or crosstalk. For comparison, red squares are conventional graphite ^{14}C values for foraminifera from Ponton et. al , 2012.

Table 1. Analysis of standards by EA-IRMS-AMS. Oxalic acid and phthalic anhydride are calibration standards for both ^{13}C and ^{14}C.

Standard	N	Mass Range (ug C)	Mean $^{12}C^{+}$ (µA)	^{14}C Consensus (Fm +- 1σ)	^{14}C Measured (Fm +- 1σ)	$\delta^{13}C$ Consensus (‰ +- 1σ)	$\delta^{13}C$ by IRMS (‰ +- 1σ)	$\delta^{13}C$ by AMS (‰ +- 1σ)
Phthalic anhydride	6	84-100	7.8	Blank[b]	0.0046 +- 0.0012	-30.01 +- 0.01[d]	-30.01 +- 0.03	-27.99 +- 2.5
Acetanilide[a]	6	104-166	7.8	0.0012 +- 0.0004	0.0023 +- 0.0014	-27.58 +- 0.02[d]	-27.57 +- 0.05	-23.65 +- 0.88
Atropine[a]	8	80-147	7.6	0.4337 +- 0.0025	0.4302 +- 0.0051	-21.43 +- 0.01[d]	-21.15 +- 0.13	-16.00 +- 2.11
IAEA-C8	8	54-83	7.5	0.1503 +- 0.0017	0.1499 +- 0.0029	-18.31 +- 0.11	-18.32 +- 0.06	-14.66 +- 1.34
Oxalic Acid	8	76-107	7.7	1.3407[c]	-	-17.68 +- 0.02[e]	-17.68 +- 0.06	-17.8 +- 2.9
IAEA-C6	8	73-130	8.0	1.5061 +-0.0011	1.5084 +- 0.0116	-10.45 +-0.03[f]	-10.50 +- 0.02	-12.17 +- 2.24

[a] In house standard, [b] For ^{14}C blank subtraction, [c] For ^{14}C normalisation, [d] From Section 3.1, [e] From Schnieder et al. Radiocarbon 1995, 37, p693, [f] From IAEA-CH6

Table S1. Calibration of Standards. Plotting measured values versus concensus for the IAEA standards gave a linear least squares fit with the equation y = 1.0152x - 0.0582 (R^2 =1) which was used to correct the unknowns for offset.

		CO2								
Id	Name	Height (nA)	$\delta^{13}C$ (VPDB)	Average	SD	Consensus	Offset	Corrected	Average	SD
6478	IAEA-CH6	55.09	-10.21			-10.45				
6479	IAEA-CH6	53.45	-10.23			-10.45				
6480	IAEA-CH6	53.39	-10.27			-10.45				
6481	IAEA-CH6	53.09	-10.27			-10.45				
6482	IAEA-CH6	52.76	-10.24			-10.45				
6485	IAEA-CH6	55.45	-10.25			-10.45				
6486	IAEA-CH6	55.20	-10.25			-10.45				
6487	IAEA-CH6	52.87	-10.27	-10.25	0.02	-10.45	-0.20			
6488	Oxalic Acid II	49.78	-17.30					-17.62		
6489	Oxalic Acid II	44.21	-17.33					-17.65		
6490	Oxalic Acid II	50.76	-17.44					-17.76		
6491	Oxalic Acid II	48.27	-17.43					-17.75		
6492	Oxalic Acid II	49.57	-17.34					-17.66		
6493	Oxalic Acid II	48.05	-17.39					-17.71		
6494	Oxalic Acid II	50.70	-17.36					-17.68		
6495	Oxalic Acid II	50.22	-17.41					-17.73		
6496	Oxalic Acid II	50.29	-17.29					-17.62		
6497	Oxalic Acid II	49.24	-17.31	-17.36	0.05			-17.63	-17.69	0.05
6498	Atropine	46.04	-21.07					-21.45		
6499	Atropine	45.86	-21.05					-21.43		
6500	Atropine	45.83	-21.08					-21.45		
6501	Atropine	46.73	-21.04					-21.42		
6502	Atropine	43.24	-21.05					-21.43		
6503	Atropine	47.44	-21.04					-21.42		
6504	Atropine	45.16	-21.03					-21.41		
6505	Atropine	43.21	-21.06					-21.43		
6506	Atropine	45.03	-21.05					-21.43		
6507	Atropine	46.87	-21.05	-21.05	0.01			-21.43	-21.43	0.01
6508	IAEA-CH3	43.21	-24.34			-24.72				
6509	IAEA-CH3	44.17	-24.31			-24.72				
6510	IAEA-CH3	44.32	-24.31			-24.72				
6511	IAEA-CH3	48.14	-24.31			-24.72				
6512	IAEA-CH3	47.75	-24.30			-24.72				
6513	IAEA-CH3	44.45	-24.34			-24.72				
6514	IAEA-CH3	44.44	-24.33			-24.72				
6515	IAEA-CH3	45.08	-24.35			-24.72				
6516	IAEA-CH3	42.91	-24.38			-24.72				
6517	IAEA-CH3	44.50	-24.36	-24.33	0.03	-24.72	-0.39			
6518	Phthalic Anhydride	52.20	-29.50					-30.00		
6519	Phthalic Anhydride	49.81	-29.49					-30.00		
6520	Phthalic Anhydride	52.40	-29.49					-30.00		
6521	Phthalic Anhydride	51.07	-29.49					-30.00		
6522	Phthalic Anhydride	51.53	-29.53					-30.04		
6523	Phthalic Anhydride	51.88	-29.50					-30.01		
6524	Phthalic Anhydride	52.58	-29.51					-30.02		
6525	Phthalic Anhydride	51.23	-29.52					-30.03		
6526	Phthalic Anhydride	54.21	-29.49					-30.00		
6527	Phthalic Anhydride	51.00	-29.49	-29.50	0.01			-30.00	-30.01	0.01
6528	IAEA-CH7	45.80	-31.60			-32.15				
6529	IAEA-CH7	45.40	-31.59			-32.15				
6530	IAEA-CH7	48.25	-31.53			-32.15				
6531	IAEA-CH7	43.81	-31.63			-32.15				
6532	IAEA-CH7	49.60	-31.61			-32.15				
6533	IAEA-CH7	42.51	-31.62			-32.15				
6534	IAEA-CH7	48.80	-31.60			-32.15				
6535	IAEA-CH7	46.68	-31.58			-32.15				
6536	IAEA-CH7	44.96	-31.56			-32.15				
6537	IAEA-CH7	47.19	-31.56	-31.59	0.03	-32.15	-0.56			
6552	Acetanilide	48.13	-27.12					-27.59		
6553	Acetanilide	50.22	-27.09					-27.56		
6554	Acetanilide	46.52	-27.11					-27.58		
6555	Acetanilide	49.09	-27.09	-27.10	0.02			-27.56	-27.58	0.02
6562	IAEA-CH6	55.10	-10.15			-10.45				
6563	IAEA-CH6	52.92	-10.17			-10.45				
6564	IAEA-CH6	49.47	-10.22			-10.45				
6565	IAEA-CH6	52.13	-10.19			-10.45				
6566	IAEA-CH6	46.66	-10.24			-10.45				
6567	IAEA-CH6	52.78	-10.20	-10.20	0.03	-10.45	-0.25			

Position A - A

EA - IRMS - AMS

CHS - Vent

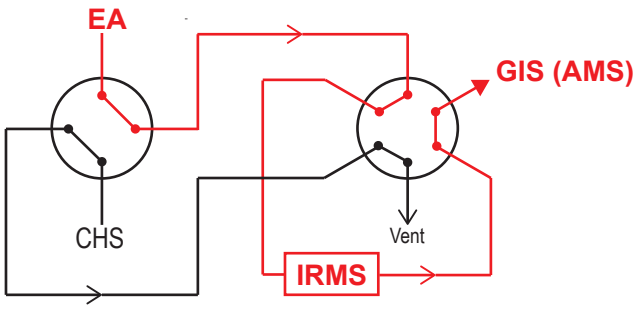

Position B - A

CHS - IRMS - AMS

EA - Vent

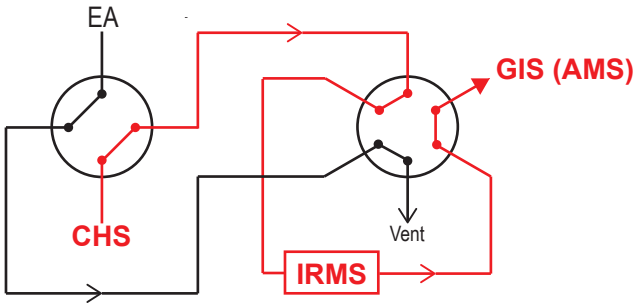

Position A - B

EA - AMS

CHS - IRMS

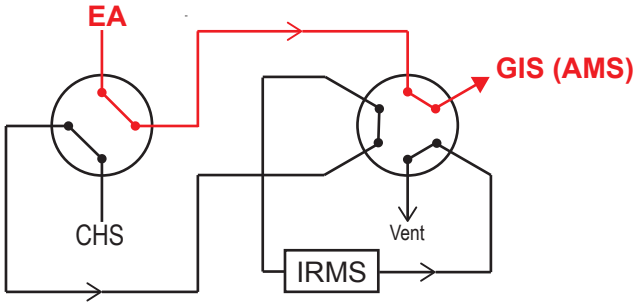

Position B - B

CHS - AMS

EA - IRMS

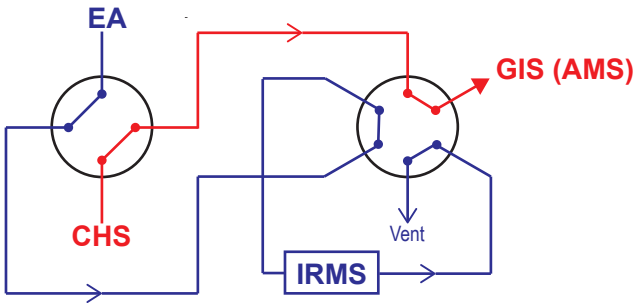

Figure S1. Schematic of the valve arrangement. Vici Valco 4-port and 6-port valves (0.75 mm bore) are used to connect the carbonate handling system (CHS) and the elemental analyser (EA) to the IRMS and AMS systems. Separate systems can then be operated concurrently. GIS (AMS) refers to the input of the GIS box.